WideBand THz Patch Antenna with Asymmetric Dielectric-Plasmonic Superconductor Waveguide

Zahra Manzoor
Department of Electrical and Computer Engineering
Missouri University of Science and Technology
Rolla, United States of America

Abstract—**In this paper, a design of end-fire modified wide band THz patch antenna is introduced by employing NbN superconductor working at 8 K in asymmetric dielectric-plasmonic waveguide. Compare to conventional design of propsed waveguides with metallic particles, utilizing superconductor particles increase antenna's bandwidth upto 12%. Furthermore, far-field radiation of the proposed design is more directive than the conventional one.**

Keywords—THz patch antenna; superconductor; plasmonic waveguide

I. INTRODUCTION

In recent years, many efforts are investigated to develop Terahertz (THz) band communication respect to its high security and wide range coverage [1]-[8]. One of the vital elements in THz wireless technology, which suffer high attenuation path loss, are antennas for broad band, low power transmissions [1], [9]-[10]. The microstrip antennas are known the most compact usable components to facilitate multi-band and/or broadband, high power and omnidirectional wireless transmission [11]. THz plasmonic antennas are nominated by [1], [12]-[13] as an interesting solution for demands of THz wireless technology. However, these types of antennas should have potential to integrate silicon photonics waveguides [2]-[8]. To this end, highly efficient hybrid plasmonic patch antennas are proposed which have the most compatibility with dielectric waveguides compare with other plasmonic designs. Hybrid patch antennas are inspired by multilayer hybrid plasmonic waveguide discussed in [4], [6]-[7] with moderate electric field confinement and propagation losses. In these structures layers are integrated on silicon-on-isolator (SOI) substrates due to their silicon-based nature and have high compatibility with conventional silicon photonic waveguides.

In this work, similar to the suggested waveguide in [6], the patch antenna integrated to asymmetric dielectric-plasmonic waveguide is designed for working at neighbor of 1 THz. However, respect to high ohmic losses of metals in THz range, the quality factor (Q-factor) of the antenna decreases. To this end, for suppressing metallic loss, metals in the asymmetric dielectric-plasmonic waveguide are replaced with superconductors, which exhibit near zero dc resistance and minimal ohmic losses at defined frequency range. This condition is achievable when superconductors are cooled down below the superconducting transition temperature (Tc) [14]. Among different superconductors, some of them such as yttrium-barium-copper oxide (YBCO) are not suitable for working at THz range regards to showing surface resistance greater than metals (e.g. copper). As discussed in [15], Nb can be nominated as the good superconductor candidate because of its low THz ohmic loss. Moreover, experiments revealed NbN superconducting can be work at higher gap frequency compare to Nb superconductors and provides structures with lower ohmic loss and higher Q-factor as well.

In this work, we present the THz patch antenna integrated to asymmetric dielectric-plasmonic waveguide covers 12% wider bandwidth when silver particles are replaced by NbN superconductor. Moreover, higher directivity (~ 4dB) is observed in radiation profile of the designed patch antenna in the presence of NbN superconductor instead of silver.

II. ANTENNA DESIGN

In Fig. 1, the schematic of proposed THz patch antenna with asymmetric integrated dielectric-plasmonic waveguide is shown when V-shaped particles are NbN superconductor working at 8 K. In [16], both real and imaginary parts of complex conductivity of the NbN film at 8 K are derived experimentally for working frequency less than 1 THz. Here, the complex permittivity is calculated from the complex conductivity by employing (1), where ω is angular frequency, σ_1, σ_2, ε_0, ε_∞ are real part of the conductivity, imaginary part of the conductivity, the dielectric constant of vacuum and optical dielectric constant, respectively [17]. Derived complex permittivity is used in modeling NbN particles in CST simulator.

$$\varepsilon = \varepsilon_1 + i\varepsilon_2 = (\varepsilon_\infty - \sigma_2/\omega\varepsilon_0) + i(\sigma_1/\omega\varepsilon_0) \quad (1)$$

These three particles are deposed inside the silica slot layer which the majority of transmitted electromagnetic fields are localized there. Also, it is expected by replacing the silver particles with NbN ones, field perturbation in the slot layer decreases dramatically [12] – [13]. Hence, unwanted radiation mostly leaked from the waveguide section reduces and as a result of this alternation, ultimate gain of the antenna increases. Moreover, this replacement causes the matching between designed waveguide and patch antenna increases and as a result, bandwidth of the antenna increases. This claim is supported by simulation results provided by CST Microwave Studio® discussed in Section III. Similar to [6] and shown in Fig. 1, the mask layer is made from silicon nitride (Si_3N_4) with $< 3 \times 10^{-3}$ loss tangent for low propagation loss compare to plasmonic waveguides suh as metal-insulator-metal (MIM) structures.

Finally, similar to [6], to control over layer's thickness precisely, metal organic chemical vapor deposition (MOCVD) can be nominated for deposition each layer [18]-[20].

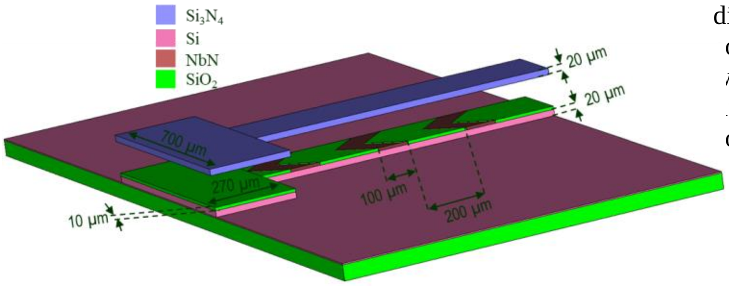

Fig. 1. Designed modified THz patch antenna with asymmetric dielectric-plasmonic waveguide employed NbN superconductor.

III. SIMULATION RESULTS

In this Section, simulations are prepared for proposed antenna model to work at 0.8- 1 THz. As discussed earlier, V-shaped particles are deposed inside the silica slab layer. By making particles from NbN instead (cooled down below Tc) of silver (Ag), it is expected the field perturbation caused by metallic nature of particles suppressed and as result, reflection coefficient (S_{11}) of the proposed design decreases in a wider frequency range compare to the design with Ag particles. In Fig. 2, $|S_{11}|$ is shown when V-shaped particles are made from Ag, NbN and SiO_2 respectively. As seen, for Ag particles, the impedance matching ($|S_{11}| < -10$ dB [21]) is less compare to two other cases and as a result, the bandwidth ($\Delta f/f_{center}$) is 10%. On the other hand, for NbN particles the matching increases and bandwidth reaches to 22%, around two times more than the one with silver (Ag) particles. This bandwidth improvement will be desired in many applications specifically imaging application respect to dependency of image resolution to imaging system's bandwidth [22]-[27]. Also, as seen, by choosing SiO_2 particles, the field perturbation is perfectly suppressed and $|S11| < -10$ dB in the whole simulated range. However, the main lobe of the far-field radiation pattern in the designed antenna deviates from Theta = 0˚ (end-fire), when particles are made from SiO_2 (shown in Fig. 3). Hence, to have directive end-fire antenna, NbN particles are chosen. In Fig. 3, far-field radiation pattern at E-plane (Phi = 0°) for the designed antenna at 0.78 THz is depicted for three different cases (Ag, NbN and SiO_2 particles). As seen, to have end-fire radiation pattern, NbN particles are better choices compare to Ag or SiO_2 particles. Moreover, the unwanted radiation leakage for the design with NbN particles is around 7 dB less than the design with SiO_2 particles (design with higher bandwidth). In Fig. 4, far-field radiation pattern at H-plane (Phi = 90°) for the designed antenna at 0.78 THz is depicted for three different cases (Ag, NbN and SiO_2 particles). Similar to E-plane simulated results, the main lobe is close to Theta = 0°, when V-shaped particles are made from NbN superconductor.

Next, the far-field radiation pattern at H-plane (Phi = 90°) for the designed antenna at 0.98 THz is illustrated in Fig. 5 for two cases (Ag and NbN particles). At this frequency (center frequency of designed antenna with Ag particles), still the end-fire main lobe of the radiation pattern is higher (around 4 dB), when NbN superconductor particles are considered for the design.

Finally, the far-field radiation pattern at E-plane is depicted in Fig. 6 at lower edge of the frequency band (0.75 THz) of the designed antenna with NbN particles for different silica slot layer's thickness. As seen, for 10 μm thickness, the directivity of the designed antenna is around 0.6 dB more ompare to directivity of the antenna with 5 μm slot layer. It is orth mentioning, increasing thickness of the slot layer (> 10 m in this case) causes reduction of the electric field onfinement in the waveguide section.

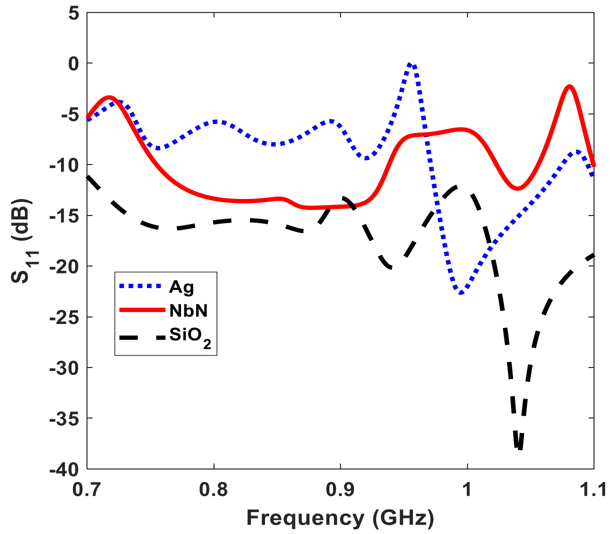

Fig. 2. Simulated $|S_{11}|$ for V-shaped particles are made from Ag, NbN and SiO_2.

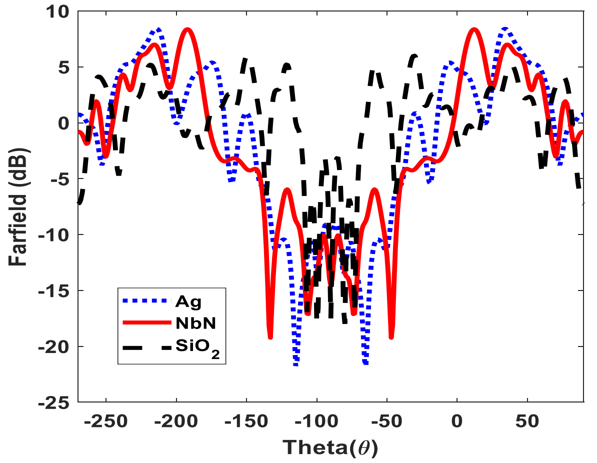

Fig. 3. Far-field radiation pattern at E-plane (Phi = 0°) for the designed antenna at 0.78 THz is depicted for three different cases (Ag, NbN and SiO2 particles).

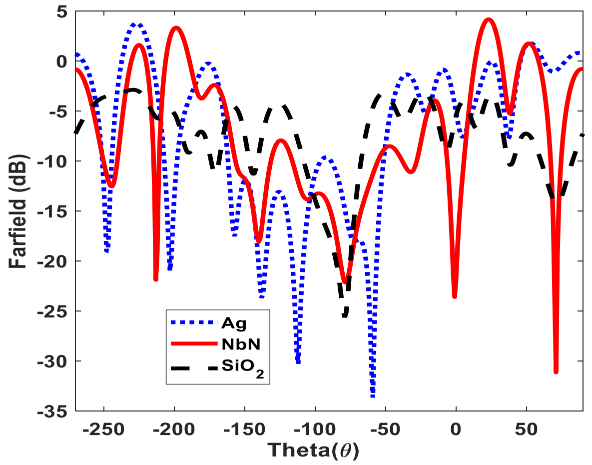

Fig. 4. Far-field radiation pattern at H-plane (Phi = 90°) for the designed antenna at 0.78 THz is depicted for three different cases (Ag, NbN and SiO2 particles).

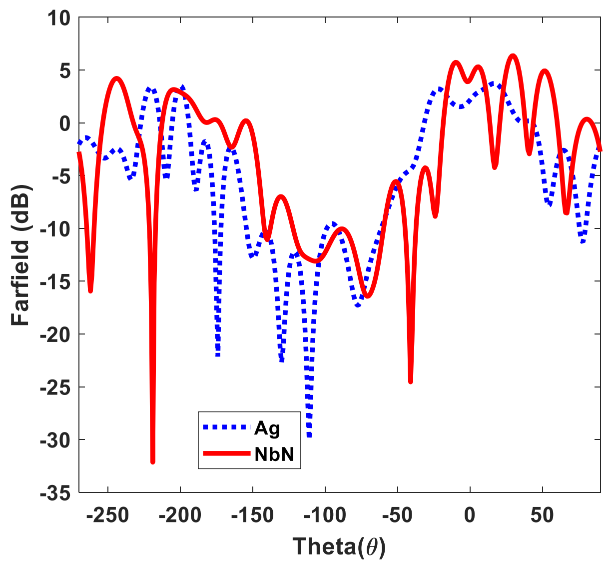

Fig. 5. Far-field radiation pattern at H-plane (Phi = 90°) for the designed antenna at 0.98 THz.

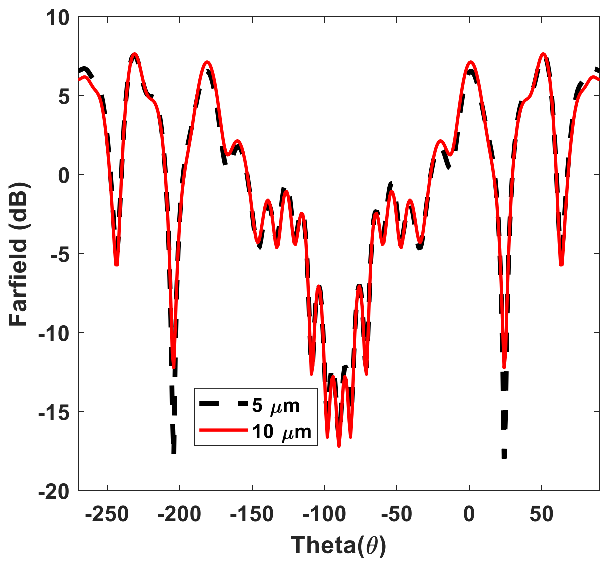

Fig. 6. Far-field radiation pattern at E-plane in lower edge of the frequency band (0.75 THz) of the designed antenna with NbN particles for different silica slot layer's thickness.

IV. CONCLUSION

In this work, modified THz patch antenna is proposed, which is fed by asymmetric dielectric-plasmonic waveguide. Unlike conventional design discussed in [6], in the new design, NbN is utilized for directive V-shaped particles and is cooled down to work as the superconductor. As a result, the bandwidth of the antenna is around 12% more than the bandwidth of the case with silver particles. This bandwidth improvement is justified based on improving matching when superconductor is employed in waveguides used for excting antennas.

REFERENCES

[1] A. Sharma, V. K. Dwivedi and G. Singh, "THz Rectangular Microstrip Patch Antenna on Multilayered Substrate for Advance Wireless Communication Systems", Proceedings of Progress in Electromagnetics Research Symposium PIERS 2009, pp. 627-631, March 23-27, 2009.

[2] Z. Manzoor, M. A. Panahi, and A. Pak, "Multicomponent-multilayer hybrid plasmonic leaky-wave optical antenna with improved directivity and matching," Terahertz, RF, Millimeter, and Submillimeter-Wave Technology and Applications XI. Vol. 10531, International Society for Optics and Photonics, 2018.

[3] L. Yousefi, "Highly directive hybrid plasmonic leaky wave optical nano-antenna," Progress In Electromagnetics Research Letters, Vol. 50, 85-90, 2014.

[4] Z. Manzoor, M. A. Panahi, and A. Pak, "Hybrid Wedge-integrated Plasmonic-photonic Waveguide," 2019 United States National Committee of URSI National Radio Science Meeting (USNC-URSI NRSM). IEEE, 2019.

[5] L. Yousefi, A. C. Foster, "Waveguide-fed optical hybrid plasmonic patch nano antenna," Opt. Exp., vol. 20, No. 16, 18326-18335, 2012.

[6] Z. Manzoor, M. A. Panahi, and A. Pak, "E-shaped Nano-antenna with Asymmetric Integrated Dielectric-plasmonic Waveguide," 2019 IEEE International Symposium on Antennas and Propagation and USNC-URSI Radio Science Meeting. IEEE, 2019.

[7] P. Sharma, and V. Dinesh Kumar, "Multilayer Hybrid Plasmonic Nano Patch Antenna," Plasmonics, Vol. 14, No. 2, 435-440, 2019.

[8] Z. Manzoor, A. Mirala, A. Pak, and M. A. Panahi, "Low loss semi-MIM hybrid plasmonic waveguide with high electric field confinement," Microwave and Optical Technology Letters, Vol. 61, No. 11, 2557-2564, 2019.

[9] Pahlavan, P., et al. "Frequency scanning in the uniform leaky-wave antenna based on nonradiative dielectric (NRD) waveguide." *2011 19th Iranian Conference on Electrical Engineering. IEEE*, 2011.

[10] Hosseini, S. R., Shirazi, R. S., Kiaee, A., Pahlavan, P., & Sorkherizi, M. S. (2012). UHF Propagation Prediction in Smooth Homogenous Earth Using Split-step Fourier Algorithm. *Progress In Electromagnetics Research*, 685, 2012.

[11] Z. Manzoor, and G. Moradi, "Optimization of Impedance Bandwidth of a Stacked Microstrip Patch Antenna with the Shape of Parasitic Patch's Slots," Applied Computational Electromagnetics Society Journal, Vol. 30, No. 9, 1014-1018, 2015.

[12] Boroomandisorkhabi, B., and R. Rahimi. "Wide Band E-Shaped Nano-Antenna with Asymmetric Hybrid Plasmonic Waveguide.", International Journal of Engineering Research & Technology (IJERT), vol. 9 Issue 07, July, 2020.

[13] Sorkhabi, Farzad Boroumandi, and Behzad Boroomandisorkhabi. "Directive Pentagon Patch Nano-Antenna for Nanofocusing Application.", International Journal of Engineering Research & Technology (IJERT),vol. 9 Issue 09, September, 2020.

[14] G. Scalari et al., "Superconducting complementary metasurfaces for THz ultrastrong light-matter coupling", New J. Phys., vol. 16, no. 3, 2014.

[15] C. H. Zhang, J. B. Wu, B. B. Jin, Z. M. Ji, L. Kang, W. W. Xu, et al., "Low-loss terahertz metamaterial from superconducting niobium nitride films", Opt. Exp., vol. 20, pp. 42-47, 2012.

[16] Wang, Dongyang, Zhen Tian, Caihong Zhang, Xiaoqing Jia, Biaobing Jin, Jianqiang Gu, Jiaguang Han, and Weili Zhang. "Terahertz superconducting metamaterials for magnetic tunability." Journal of Optics 16, no. 9, 094013, 2014.

[17] Kalhor, S., et al. "Data supporting" Thermal Tuning of High-Tc Superconducting Bi2Sr2CaCu2O8+ δ Terahertz Metamaterial".", *IEEE Photonics Journal IEEE Photonics Journal*, DOI 10.1109/JPHOT.2017.2754465, 2020.

[18] V. Saravade, Z. Manzoor, A. Corda, C. Zhou, and N. Lu, "Nickel doping in zinc oxide by MOCVD: structural and optical properties," Quantum Sensing and Nano Electronics and Photonics XVII., Vol. 11288, International Society for Optics and Photonics, 2020.

[19] Manzoor, Z., Saravade, V., Corda, A. M., Ferguson, I., & Lu, N., Optical and structural properties of nickel doped zinc oxide grown by metal organic chemical vapor deposition (MOCVD) at different reaction chamber conditions. *ES Materials & Manufacturing*, 8, 31-35, 2020.

[20] Saravade, V., Manzoor, Z., Corda, A., Zhou, C., Ferguson, I., & Lu, N., Optical and Structural Properties of Manganese-Doped Zinc Oxide Grown by Metal-Organic Chemical Vapor Deposition. *Advanced Optical Materials*, 2100096, 2021.

[21] Manzoor, Zahra. "Polarisation detection sensor with EO polymer-dispersed liquid crystals." Electronics Letters 56, no. 1, 9-11, 2020.

[22] Z. Manzoor, M. T. A. Qaseer and K. M. Donnell, "A Comprehensive Bi-Static Amplitude Compensated Range Migration Algorithm (AC-RMA)," *IEEE Transactions on Image Processing*, vol. 30, pp. 7038-7049, 2021, doi: 10.1109/TIP.2021.3100679.

International Journal of Engineering Research & Technology (IJERT)
ISSN: 2278-0181
Vol. 10 Issue 11, November-2021

[23] Manzoor, Zahra, A. Mohammad Tayeb Al Qaseer, and Kristen M. Donnell. "Improved grounded coplanar waveguide-to-multilayer substrate integrated waveguide transition for efficient feeding of an antipodal Vivaldi antenna for imaging applications." *Microwave and Optical Technology Letters*, 63.6, 1712-1718, 2021.

[24] Manzoor Z., "Aperiodic Hyperbolic Metamaterial Superlens with Random Distribution.", *Optik*. 2021, 167290, May, 2021.

[25] Manzoor, Zahra, and Sajjad Taravati. "Enhanced resolution imaging by aperiodically perturbed photonic time crystals." *2020 Conference on Lasers and Electro-Optics (CLEO)*. IEEE, 2020.

[26] Manzoor, Zahra. "Polarisation detection sensor with EO polymer-dispersed liquid crystals." *Electronics Letters* 56, no. 1, 9-11, 2020.

[27] Manzoor, Zahra. "Polarisation detection sensor with EO polymer-dispersed liquid crystals." Electronics Letters 56, no. 1, 9-11, 2020.